

# Non-Fermi liquid properties of $2d$ symplectic fermions: the role of a dynamically generated (pseudo)-gap

Eliot Kapit and André LeClair

*Newman Laboratory, Cornell University, Ithaca, NY*

## Abstract

The interacting symplectic fermion model in two spatial dimensions is further analyzed. As an effective low energy theory, the model is unitary. We show that a relativistic mass  $m$  is dynamically generated and derive a gap equation for it. By incorporating a finite temperature we study some fundamental properties of the model, such as the specific heat and spin response, which clearly show non-Fermi liquid properties. We find that various physical properties are suppressed at temperatures  $T < T^*$  where the cross-over scale is  $T^* = m$ . As a simplified, toy model of high  $T_c$  superconductivity, we thus identify the pseudogap energy scale with the zero temperature relativistic mass  $m$ , and show that this reproduces some qualitative aspects of the observed phenomenology of the pseudogap. The effects of the pseudogap and finite temperature on the d-wave gap equation are analyzed. In this model, the pseudogap is a distinct phenomenon from superconductivity and in fact competes with it. Our analysis of  $T_c$  suggests that the quantum critical point of our model, where the pseudogap vanishes, occurs inside the superconducting dome near optimal doping. For an antiferromagnetic exchange energy of  $J/k_B \sim 1350K$ , solutions of the d-wave gap equation give a maximum  $T_c$  of about  $110K$ .

## I. INTRODUCTION

An important aspect of strongly-correlated electron physics is the expectation that some systems may exhibit novel non-Fermi liquid behavior. This can present some interesting challenges for theoretical models since non-Fermi liquid behavior is known to be rare based on simple renormalization group (RG) arguments[1]. The best understood example is the Luttinger liquid in one spatial dimension, where the non-Fermi liquid behavior is essentially attributed to the fact that quartic interactions of Dirac fermions are marginal in the RG sense. In higher dimensions quartic interactions of Dirac fermions are irrelevant. These considerations were one of the primary initial motivations for the construction and analysis of a new model of interacting fermions[2, 3, 4] with non-Fermi liquid behavior. Like the Luttinger liquid, the model is a continuum field theory of only 4 fermionic fields  $\chi_{\uparrow,\downarrow}^{\pm}$  which carry charge and spin, with a unique quartic interaction due to Fermi statistics. The novelty of the model is the free kinetic term in the hamiltonian which in addition the commonplace term that is second order in spatial derivatives  $\vec{\nabla}\chi^{-} \cdot \vec{\nabla}\chi^{+}$ , contains an additional contribution that is second order in time derivatives  $\partial_t\chi^{-}\partial_t\chi^{+}$ , and thus has an emergent Lorentz symmetry. The model can be consistently canonically quantized as a fermion, even though this structure of the kinetic term is usually associated with relativistic bosons. In two spatial dimensions the field  $\chi$  has dimension 1/2, which implies the quartic interaction has dimension 2 and is thus RG relevant. The model in fact has a low-energy fixed point, i.e. quantum critical point.

Several interesting properties in addition to the non-Fermi liquid behavior emerged in the analysis of the model[4]. It has a hidden  $SO(5)$  symmetry which contains the spin  $SO(3)$  and electric  $U(1)$  as commuting subgroups. The fundamental fields  $\chi_{\uparrow,\downarrow}^{\pm}$  transform in the 4-dimensional spinor representation of  $SO(5)$  and the bilinears decompose as  $\mathbf{4} \otimes \mathbf{4} = \mathbf{1} \oplus \mathbf{5} \oplus \mathbf{10}$ . The  $\mathbf{5}$  vector representation serves as order parameters for the spontaneous symmetry breaking of  $SO(3)$ , i.e. magnetic order, and also contains Cooper pair fields of charge  $\pm 2$  which are order parameters for symmetry breaking of  $U(1)$ , i.e. superconductivity. By deriving separate gap equations and studying their solutions it was shown that the model can contain an anti-ferromagnetic phase (AF) and a d-wave superconducting phase (SC). In this model the basic mechanism that leads to a d-wave SC instability is clearly identified as arising from the 1-loop scattering of Cooper pairs. An attractive feature of the model is its

simplicity, reflected in the fact that it has very few free parameters: an overall energy scale  $E_0$  set by the high-energy cutoff  $\Lambda_c$ , a Fermi velocity  $v_F$ , and a single coupling  $g$ . Furthermore, at low energies  $g$  is near the low-energy fixed point value of  $1/8$ , so that perturbation theory can be reliable.

The above features led us to propose this theory as a toy model of high temperature superconductivity (HTSC). Here the  $SO(5)$  symmetry is quite different from the  $SO(5)$  symmetry of Zhang in this context[5]: whereas he postulates an  $SO(5)$  invariant Landau-Ginsburg theory for the bosonic spin and electric order parameters, our model is a microscopic model of fermions where the bosonic order parameters are composite bilinears in the fermions. The  $SO(5)$  symmetry was not put in by hand in our model, rather it is accidental and hidden. In fact, the AF and d-wave SC phases are *not* related by the  $SO(5)$  in our model. In principle a Landau-Ginsburg effective theory can be derived from our model, but like the BCS theory, our underlying microscopic theory is more powerful for deriving gap equations, critical temperatures, etc. Arguments that motivate its application to HTSC were given in [4], the best one being its relation to the non-linear  $O(3)$  sigma model effective theory for the  $2d$  Heisenberg model description of the AF phase, which is also a relativistic theory; however a rigorous derivation of it from say the Hubbard model on the lattice is lacking. If our model really turns out to correctly capture some essential features of HTSC, then it should be viewed as an effective low-energy theory for wavelengths that are long compared to the lattice spacing. One expects that such a description can be approximately described by a rotationally invariant quantum field theory describing the gas of quasi-particles that SC condenses out of. The shortcoming of such a theory is that lattice effects, such as features that are dependent on the detailed structure of the Fermi surface in the Brillouin zone, are necessarily absent in the basic model, although perhaps they can be incorporated with small perturbations of the hamiltonian. Furthermore, our model does not have an explicit Fermi surface, as for the  $O(3)$  sigma model of the AF phase at half-filling. Nevertheless, the existence of a simple model of fermions with only repulsive quartic interactions that possesses the all of the main motifs of HTSC, which is to say it has clearly identified mechanisms for the d-wave SC, the pseudogap, and anti-ferromagnetism, can be useful for deciding which properties are essential and which are superfluous for the phenomenon. Thus, although it has not been established that our model captures what is really happening in HTSC, for the remainder of this paper we will take the liberty to borrow the terminology of the HTSC

literature where appropriate.

The main purpose of the present article is study in detail the origin and properties of the so-called pseudogap in our model. In the HTSC materials, the pseudogap refers to an energy scale  $E_{pg} \equiv k_B T^*$  where a cross-over behavior is observed in a variety of physical properties such as electronic specific heat, magnetic susceptibility and conductivity. The same energy scale can be observed as the onset of a depression in the density of states. In the underdoped region,  $T^*$  is considerably larger than the superconducting  $T_c$ . For reviews see [6, 7]. The origin and physical interpretation of the pseudogap remains a fundamental question in the physics of HTSC, and many researchers feel that a proper understanding of it will be an important key toward unraveling the mysteries of HTSC. Two broad classes of theories can be summarized by the schematic phase diagrams shown in Figure 1. In the scenario on the left,  $T^*$  goes to zero inside the SC dome, perhaps terminating at a quantum critical point. In this class of theories the pseudogap is unrelated, and in fact competes with, superconductivity. In the second class of theories, the pseudogap indicates pre-formed Cooper pairs for example, i.e. is a friendly precursor to SC, and the pseudogap line merges with  $T_c$  on the overdoped side. These opposing scenarios are discussed in some detail in [8]. Thermodynamic data such as specific heat favors the first scenario[9, 10], whereas spectroscopic data seems to support the second[11].

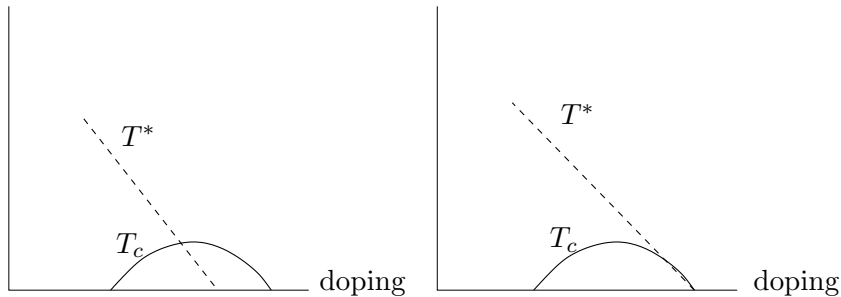


FIG. 1: Two proposed theoretical scenarios for the HTSC phase diagram.

In our model there is an obvious identification of the pseudogap: whereas AF or SC order are related to the order parameters in the  $\mathbf{5}$  vector of  $SO(5)$ , the pseudogap is naturally associated with the singlet bilinear in the tensor product of  $\mathbf{4} \otimes \mathbf{4}$ , as suggested by Tye[12], and also more tentatively in [4]. This corresponds to the operator  $\chi^- \chi^+ \equiv \sum_{\alpha=\uparrow,\downarrow} \chi_{\alpha}^- \chi_{\alpha}^+$ . Whereas this term is classically zero in the relation with the  $O(3)$  sigma model, it is dynamically generated in the presence of interactions. As a contribution to the hamiltonian, it

corresponds to a relativistic mass  $m$ , and the 1-particle states have energy  $E_{\mathbf{k}} = \sqrt{\mathbf{k}^2 + m^2}$ . Thus a non-zero mass  $m$  gives a clean gap in the density of states, i.e. there is nothing “pseudo” about it. As discussed above, the anisotropy of the observed pseudogap is not a feature of this mass-gap since it is a lattice effect (“Fermi arcs”). In the sequel we identify this mass with the pseudogap energy scale  $E_{pg} = T^* = m$  and will show that its properties closely parallel the phenomenology of the pseudogap in HTSC, at least on the underdoped side.

The pseudogap has an entirely different origin than the SC gap in our model, essentially because it corresponds to a dynamically generated vacuum expectation value  $\langle \chi^- \chi^+ \rangle$  which preserves the  $SO(5)$  symmetry whereas SC breaks the electric  $U(1)$  subgroup. It is an intrinsic property of the normal state density of states. Whether it competes with or aids superconductivity is straightforwardly addressed by incorporating it into the d-wave gap equation derived in [4]. As we will see, it clearly competes with superconductivity since if it is too large it destroys the solution to the SC gap equation. Fortunately, the pseudogap goes to zero at the critical point and this makes superconductivity possible; in fact SC is enhanced near the critical point. Thus our model is in the class of the left figure in Figure 1, with  $T^*$  terminating at a quantum critical point near optimal doping. (The proper treatment of temperature presented in this paper led to the identification of the critical point which differs from the original proposal in [4].)

Our analysis of the pseudogap required two technical improvements of the work presented in [4]. In the latter work, temperature was treated crudely as a mass, the idea being that temperature and a mass can both be viewed as an infra-red cutoff; this is ultimately unreliable for the computation of thermodynamic properties. In the present work, since the mass is identified with the pseudogap which is a zero temperature property, temperature must be dealt with properly, and this is accomplished with the Matsubara formalism. A non-zero mass also resolves some infra-red divergences that were present in the previous treatment.

The remainder of this article is organized as follows. In the next section we review the definition of the model and some of its basic properties. Section III addresses the unitarity of the model, beyond what is contained in our previous work. Section IV describes our RG prescriptions. In section V we analyze the dynamical generation of a mass, i.e. pseudogap, by deriving a gap equation for the vacuum expectation value  $\langle \chi^- \chi^+ \rangle$ . The pseudogap

depends on the variable  $x$  which up to a scale is the inverse coupling. In section VI we propose a relation between the variable  $x$  and hole doping which thus gives the doping dependence of the pseudogap. In section VII we compute the effect of the pseudogap on the electronic specific heat. A non-zero magnetic field is introduced in section VIII, and we compute the temperature dependent spin susceptibility and the magnetic field dependence of the specific heat. For all of these thermodynamic properties, we find crossover behavior at the temperature  $T = T^*$  and its qualitative dependence on doping compares favorably with data. Finally in section IX we derive the finite temperature version of the d-wave gap equation and incorporate the effect of the pseudogap into it. Analysis of this equation clearly shows that the pseudogap competes with SC, and leads to a computation of the superconducting  $T_c$ .

## II. REVIEW OF THE MODEL, IT'S SYMMETRIES AND ORDER PARAMETERS

As for any second-quantized description of electrons with spin  $\frac{1}{2}$ , the fundamental fields of the model are 4 fermionic fields  $\chi_\alpha^\pm$ , where the flavor index  $\alpha = \uparrow, \downarrow$  corresponds to spin and  $\pm$  is electric charge. Due to the fermionic statistics there is a unique quartic interaction, thus various models are primarily characterized by the free kinetic term. Our model in two spatial dimensions is

$$H = \int d^2\mathbf{x} \left( \sum_{\alpha=\uparrow,\downarrow} (\partial_t \chi_\alpha^- \partial_t \chi_\alpha^+ + v_F^2 \vec{\nabla} \chi_\alpha^- \cdot \vec{\nabla} \chi_\alpha^+ + m^2 \chi_\alpha^- \chi_\alpha^+) + 8\pi^2 g \chi_\uparrow^- \chi_\uparrow^+ \chi_\downarrow^- \chi_\downarrow^+ \right) \quad (1)$$

The above hamiltonian would be a standard second-quantized field theory for fermions interacting via a delta-function potential if it weren't for the term that is second order in time derivatives, and this is the primary novelty of the model. This choice of kinetic term can be motivated from the phenomenology of HTSC, since it leads to the correct temperature dependence of the specific heat  $C \propto T^2$  at low temperatures (see section VII) in the absence of superconductivity, which is characteristic of a relativistic theory, and the mass  $m$  can correspond to the pseudogap.

As a model of HTSC, the above kinetic term can also be motivated as follows[4]. Suppose one is near the Mott-Hubbard insulating phase. The anti-ferromagnetic phase of the Heisenberg model has an effective low energy description in terms of a spin 3-vector field

$\vec{\phi}$  constrained to be of fixed length  $\vec{\phi} \cdot \vec{\phi} = \text{constant}$ , with lagrangian  $\partial_\mu \vec{\phi} \cdot \partial_\mu \vec{\phi}$ [18, 19]. The field  $\vec{\phi}$  is bilinear in the fundamental electron fields, and in our model corresponds to  $\vec{\phi} = \chi^- \vec{\sigma} \chi^+ / \sqrt{2}$ . The constraint on  $\vec{\phi}$  can be imposed by the constraint  $\chi^- \chi^+ = \text{constant}$  since

$$\vec{\phi} \cdot \vec{\phi} = -\frac{3}{2} (\chi^- \chi^+)^2 \quad (2)$$

Imposing these constraints one finds that

$$\partial_\mu \vec{\phi} \cdot \partial_\mu \vec{\phi} \propto \partial_\mu \chi^- \partial_\mu \chi^+ + \text{irrelevant operators} \quad (3)$$

which justifies the kinetic term in our model. One can then relax the constraint on  $\chi^- \chi^+$ , and replacing it with a “soft constraint” by including a quartic interaction, as is done for the non-linear  $O(3)$  sigma model in two spatial dimensions.

Another motivation for the kinetic term in our model (at  $m = 0$ ) was given in [4] based on the linear dispersion relation  $E_{\mathbf{k}} = |\mathbf{k}|$  one obtains when expanding around a circular Fermi surface. However this involved a modification of, or at best a crude approximation to, the density of states.

Canonical quantization and also a path-integral formulation follow from the euclidean action:

$$S = \int d^2 \mathbf{x} dt \left( \sum_{\alpha=\uparrow, \downarrow} (\partial_\mu \chi_\alpha^- \partial_\mu \chi_\alpha^+ + m^2 \chi_\alpha^- \chi_\alpha^+) - 8\pi^2 g \chi_\uparrow^- \chi_\uparrow^+ \chi_\downarrow^- \chi_\downarrow^+ \right) \quad (4)$$

where  $\partial_\mu \partial_\mu = \partial_t^2 + v_F^2 \vec{\nabla}^2$ . The velocity  $v_F$  plays the role of the speed of light, and it was proposed in [4] that it be identified with the universal nodal Fermi velocity[13]. In the sequel we set  $v_F = \hbar = k_B = 1$  except where indicated. Note that the fields  $\chi$  are treated as Lorentz scalars and spin is simply a flavor. However it is possible to treat the fields as Dirac spinors and thereby achieve complete Lorentz invariance[14]. The quartic term is unique up to the sign of the coupling by fermionic statistics, and positive  $g$  corresponds to repulsive interactions.

A consequence of the fermionic statistics is that the model has a hidden  $SO(5)$  symmetry. As explained in the Introduction, the appearance of this  $SO(5)$  is quite different from the  $SO(5)$  symmetry proposed by Zhang. This symmetry is manifest if one considers an  $N$ -component version with fields  $\chi_\alpha^\pm$ ,  $\alpha = 1, \dots, N$ , which has  $Sp(2N)$  symmetry (hence the terminology “symplectic fermions”). For  $N = 2$ , since there are 4 fermionic fields and

consequently a unique 4-fermion interaction, the theory automatically has  $Sp(4) = SO(5)$  symmetry.

The  $SO(5)$  contains  $SO(3)$  and  $U(1)$  subgroups which commute and can be identified with spin and electric charge respectively. The conserved electric current then corresponds to

$$J_\mu^e = -i \sum_\alpha (\chi_\alpha^- \partial_\mu \chi_\alpha^+ + \chi_\alpha^+ \partial_\mu \chi_\alpha^-) \quad (5)$$

and the fields  $\chi^\pm$  have electric charge  $Q_e = \pm 1$ .

The important order parameters for the study of spontaneous symmetry breaking are composite bilinears in the fermions. The 4 fields  $\chi_\alpha^\pm$  transform under the spinor representation of  $SO(5)$ . The bilinears can be decomposed as  $\mathbf{4} \otimes \mathbf{4} = \mathbf{1} \oplus \mathbf{5} \oplus \mathbf{10}$  where  $\mathbf{1}$  is the singlet,  $\mathbf{5}$  the vector representation, and  $\mathbf{10}$  the adjoint. The singlet is the field  $\sum_\alpha \chi_\alpha^- \chi_\alpha^+ \equiv \chi^- \chi^+$  and corresponds to the mass term in the action. The  $\mathbf{5}$ -vector of fields corresponds to

$$\vec{\Phi} = (\vec{\phi}, \phi_e^+, \phi_e^-) = \left( \frac{1}{\sqrt{2}} \chi^- \vec{\sigma} \chi^+, \chi_\uparrow^+ \chi_\downarrow^+, \chi_\downarrow^- \chi_\uparrow^- \right) \quad (6)$$

where  $\vec{\sigma}$  are Pauli matrices. The triplet of fields  $\vec{\phi}$  are electrically neutral and transform as a spin vector under the  $SO(3)$  and serve as magnetic order parameters. The fields  $\phi_e^\pm$  on the other hand are spin singlets but carry electric charge  $\pm 2$  and are thus Cooper pair fields for superconducting order. The  $SO(5)$  invariant product is

$$\vec{\Phi} \cdot \vec{\Phi} = \vec{\phi} \cdot \vec{\phi} - 2\phi_e^+ \phi_e^- \quad (7)$$

and the interaction can be expressed in the manifestly  $SO(5)$  invariant manner:

$$\mathcal{L}_{\text{int}} = \frac{8\pi^2}{5} g \vec{\Phi} \cdot \vec{\Phi} \quad (8)$$

The momentum expansion of the free fields is

$$\begin{aligned} \chi^-(\mathbf{x}, t) &= \int \frac{d^2\mathbf{k}}{(2\pi)^2 \sqrt{2\omega_{\mathbf{k}}}} \left( a_{\mathbf{k}}^\dagger e^{-ik \cdot x} + b_{\mathbf{k}} e^{ik \cdot x} \right) \\ \chi^+(\mathbf{x}, t) &= \int \frac{d^2\mathbf{k}}{(2\pi)^2 \sqrt{2\omega_{\mathbf{k}}}} \left( -b_{\mathbf{k}}^\dagger e^{-ik \cdot x} + a_{\mathbf{k}} e^{ik \cdot x} \right) \end{aligned} \quad (9)$$

where  $\omega_{\mathbf{k}} = \sqrt{\mathbf{k}^2 + m^2}$  and  $k \cdot x = \omega_{\mathbf{k}} t - \mathbf{k} \cdot \mathbf{x}$ . The canonical quantization of the theory based on the lagrangian leads to the canonical anti-commutations in momentum space:

$$\{a_{\mathbf{k}}, a_{\mathbf{k}'}^\dagger\} = \{b_{\mathbf{k}}, b_{\mathbf{k}'}^\dagger\} = (2\pi)^2 \delta(\mathbf{k} - \mathbf{k}') \quad (10)$$



and the hamiltonian is

$$H_{\text{free}} = \int \frac{d^2\mathbf{k}}{(2\pi)^2} \sum_{\alpha=\uparrow,\downarrow} \omega_{\mathbf{k}} \left( a_{\mathbf{k},\alpha}^\dagger a_{\mathbf{k},\alpha} + b_{\mathbf{k},\alpha}^\dagger b_{\mathbf{k},\alpha} \right) \quad (11)$$

The  $a$  and  $b$  particles have opposite electric charge and can thus be thought of as particles and holes.

A distinguishing feature of our model, in contrast to quartic interactions of Dirac fermions for instance, is that the quartic interaction is relevant in the renormalization group (RG) sense: the field  $\chi$  has classical mass dimension  $1/2$  so that the quartic interaction has dimension  $2$  and the coupling  $g$  dimension  $1$ . This means that the interactions are important at low energies and can lead to non-Fermi liquid behavior. In fact, the model has a low energy RG fixed point, i.e. a quantum critical point at  $g \approx 1/8$ . This critical point can formally be understood as an analytic continuation of the familiar Wilson-Fisher fixed point of the  $O(N)$  models, where  $N = -4$ , and some critical exponents, such as the anomalous dimension of the field  $\chi$ , can be computed by specializing the known epsilon-expansion results for the  $O(N)$  model to  $N = -4$ [3]. However, many of the important operators such as the order parameters  $\vec{\Phi}$  are composite fermion bilinears, which changes their structure compared to the magnetic order parameters of the  $O(N)$  models. Furthermore,  $\vec{\Phi}$  includes bilinear order parameters of charge  $\pm 2$  that have no counterpart in  $O(N)$  physics. These RG properties are summarized in the next section.

Another interesting feature of our model is that whereas the fundamental interaction is repulsive, when one incorporates the momentum-dependent scattering at second order in perturbation theory (1-loop) there is an instability toward the formation of a d-wave superconducting ground state. This was studied in [4] by deriving a d-wave gap equation for momentum-dependent vacuum expectation values for the Cooper-pair fields  $\phi_e^\pm$ . This is reviewed briefly in section IX where we derive and study the finite temperature version of the d-wave gap equation.

### III. UNITARITY OF THE MODEL AS AN EFFECTIVE LOW ENERGY THEORY.

The above free hamiltonian (11) in momentum space is obviously hermitian and defines a unitary theory, in spite of the fact that the Klein-Gordon type of action normally associated

with free bosons was quantized with the “wrong” statistics, i.e. as a fermion. There are no negative norm states in the Fock space of  $a, b$  particles since there are no unwanted minus signs in eq. (10). In  $1d$  the free massless symplectic fermion model is normally considered a non-unitary  $c = -2$  conformal field theory. The resolution of this apparent contradiction can be found in [17], where it was shown that the symplectic fermion can be mapped onto the  $c = 1$  unitary theory[17] of Dirac fermions at the level of detailed conformal partition functions. In light of the above results, the latter fact is not surprising since in momentum space the hamiltonians of symplectic and Dirac fermions are identically eq. (11).

The issue of unitarity was further addressed in [3, 4], where the main concern is the consistency of the interacting theory. Because of the extra minus sign in (9), the fields  $\chi^\pm$  are not hermitian conjugates of each other, but rather

$$\chi^+ = C(\chi^-)^\dagger C \quad (12)$$

where the unitary operator  $C$  simply distinguishes particles and holes:  $CaC = a$  and  $CbC = -b$ , with  $C^\dagger C = C^2 = 1$ . The operator  $C$  is easily constructed:

$$C = \exp \left( i\pi \int \frac{d^2\mathbf{k}}{(2\pi)^2} \sum_\alpha b_{\mathbf{k},\alpha}^\dagger b_{\mathbf{k},\alpha} \right) \quad (13)$$

The interacting theory is thus pseudo-hermitian:  $H^\dagger = CHC$ . The free theory is actually hermitian in momentum space since it is quadratic in  $b$ 's. As before there are no negative norm states in the Fock space.

A pseudo-hermitian hamiltonian has real energy eigenvalues, and can still lead to a unitary time evolution, as discussed in [3, 4, 15, 16]. Let us make the following additional remarks concerning this issue in this specific context. A unitary time evolution follows if one modifies the definition of hermitian conjugation. Define the  $C$ -hermitian conjugate as  $A^{\dagger c} = CA^\dagger C$ . Then the S-matrix is unitary with respect to this conjugation:  $S^{\dagger c} S = 1$  since  $H^{\dagger c} = H$ . However the  $C$ -conjugate hermitian conjugation implies a modified definition of the inner product:  $\langle \psi' | \psi \rangle \rightarrow \langle \psi' | \psi \rangle_c \equiv \langle \psi' | C | \psi \rangle$ . Under this new inner product, states with an odd number of  $b$  particles now have negative norm. A completely equivalent description that dispenses altogether with the operator  $C$  amounts to removing the minus sign in the expansion of  $\chi^+$  in eq. (9). This gives a hermitian hamiltonian since now  $\chi^- = (\chi^+)^\dagger$ . However this also gives the modified relation  $\{b_{\mathbf{k}}, b_{\mathbf{k}'}^\dagger\} = -(2\pi)^2 \delta(\mathbf{k} - \mathbf{k}')$  and this leads to the same conclusion that the  $b$  particle sector contains negative norm states.

We now argue that this model can still yield a consistent theory at *low energy*. Let us use the description based on the  $C$ -operator; the same arguments apply to the manifestly hermitian description without it. The probability that an initial state  $|i\rangle$  evolves to a final state  $|f\rangle$  is given by

$$P_{if} = \frac{|\langle i|S|f\rangle_c|^2}{\langle i|i\rangle_c \langle f|f\rangle_c} \quad (14)$$

States can be classified according to their  $C$  eigenvalue of  $\pm 1$ , where  $C = -1$  corresponds to negative norm. One sees from the above formula that the probability  $P_{if}$  is positive so long as the states  $|i\rangle, |f\rangle$  are both of either positive or negative norm. The problematic transitions with negative probability thus arise if the matrix element  $\langle i|S|f\rangle$  is non-zero for states of mixed norm. However at low energies compared to the mass  $m$ , these transitions are forbidden as a result of energy and charge conservation. For example, suppose the initial state consists of only  $a$ -particles. Because of charge conservation, processes that change the number of  $b$  particles necessarily involve creation of  $a, b$  pairs; for instance  $aa \rightarrow ab$  is not allowed. The process  $a \rightarrow aab$  is consistent with charge conservation, but not allowed kinematically, so one needs to consider at least  $aa \rightarrow aaab$ . Energy conservation shows that the energy of the initial  $a$  particles must be at least  $2m$  in order for the process to be kinematically allowed. Thus at low energies compared to the mass  $m$  no  $b$ -particles will be produced from a state containing only  $a$  particles. A variation of this viewpoint interchanges the role of  $b$  and  $b^\dagger$ , so that particles are created by the  $b$ 's and have negative energy. One can now imagine that all the negative energy states are filled according to the Pauli principle. Since there is a gap of  $2m$  between the negative and positive energy states, at low energies compared to  $m$  no  $ab$  pairs will be created out of the Dirac sea and one can deal only with the  $a$ -particles.

As we describe in the sequel, the mass  $m$  is on the order of the cut-off and can be quite large, typically greater than  $1000K$  for HTSC materials, so the low energy approximation is expected to be good for a large range of temperatures. At very high temperatures, our model necessarily breaks down and must be replaced by another effective theory that restores unitarity. For instance, the cross-over to ordinary Fermi liquid behavior in for example the specific heat is not built into the model.

Another way to obtain a low energy unitary theory involves the introduction of a chemical potential, which is necessary at finite density. Particle number is not conserved here; instead a chemical potential couples to the electric charge  $Q_e$ , i.e.  $H \rightarrow H + \mu Q_e$ . The free

hamiltonian is then

$$H = \int \frac{d^2\mathbf{k}}{(2\pi)^2} \left( (\omega_{\mathbf{k}} + \mu) a_{\mathbf{k}}^\dagger a_{\mathbf{k}} + (\omega_{\mathbf{k}} - \mu) b_{\mathbf{k}}^\dagger b_{\mathbf{k}} \right) \quad (15)$$

Because of the difference in electric charge between the  $a$  and  $b$  particles, at a given  $\mathbf{k}$  there is a gap of  $2\mu$  between the energies of the  $a$ 's and  $b$ 's. Let us suppose that  $\mu$  is chosen so that all of the  $b$ -states are filled. Typically  $\mu$  will be comparable to the Fermi energy and typically very large. If  $\mu$  is large enough, then because of the energy gap  $2\mu$  at low energies we can effectively deal only with the  $a$ -particle sector. Alternatively, one can view the  $a$  sector as an in-accessible high energy sector when  $\mu$  is large enough, and deal only with the low-energy  $b$  sector. Either way, as discussed above, all probabilities  $P_{if}$  will be positive.

#### IV. RENORMALIZATION GROUP PRESCRIPTIONS

In all approaches to the renormalization group there are two cut-offs, a fixed upper cut-off  $\Lambda_c$  typically related to the inverse lattice spacing, and a lower cut-off  $\Lambda < \Lambda_c$  which is the running RG scale. Renormalization effectively removes the degrees of freedom with energy between  $\Lambda$  and  $\Lambda_c$ . In the high-energy physics context, the cut-off  $\Lambda_c$  is unknown, so one normally performs the renormalization by sending  $\Lambda_c$  to infinity and incorporating counter-terms to cancel ultra-violet divergences. In  $D = 4$  spacetime dimensions this can be conveniently and systematically performed by using dimensional regularization in  $D = 4 - \epsilon$  dimensions, which leads to the epsilon-expansion technique for studying models in  $D = 3$ . In the present context, since the cut-off  $\Lambda_c$  is in principle known and physical quantities depend on it, it is more appropriate to perform the RG directly in  $D = 3$  with explicit cut-offs rather than use the epsilon expansion.

The dependence of the couplings on the running RG scale  $\Lambda$  can be determined by considering an upper cut-off  $\Lambda$  only. Consider first the coupling constant  $g$ . The 1-loop correction to the vertex is cancelled by a shift of  $g$ , i.e. by defining  $g(\Lambda) = g + \delta g$  where

$$\delta g = 16\pi^2 g^2 \int^\Lambda \frac{d^3\ell}{(2\pi)^3} \frac{1}{(\ell^2 + m^2)^2} \quad (16)$$

When  $\Lambda \gg m$ ,  $g(\Lambda) = g - 8g^2/\Lambda$ . Thus

$$\Lambda \partial_\Lambda g(\Lambda) = \frac{8g^2}{\Lambda} \quad (17)$$

Let us define

$$g = \Lambda \hat{g} \quad (18)$$

Then the beta function for the dimensionless coupling  $\hat{g}$  is

$$\Lambda \partial_\Lambda \hat{g} = -\hat{g} + 8\hat{g}^2 \quad (19)$$

The above beta-function eq. (19) has a low energy fixed point at  $\hat{g} = 1/8$ . It is known that this fixed point survives, with small corrections, to higher orders[3]. We can now integrate the RG flow and incorporate the initial data at the high energy cut-off  $\Lambda_c$ . It will be convenient to introduce the dimensionless variable  $x$ :

$$x \equiv 1/\hat{g} \quad (20)$$

The fixed point occurs at  $x_* = 8$ . Let  $\hat{g}_0$  be the value of the coupling at the scale  $\Lambda_c$ , and  $x_0 = 1/\hat{g}_0$ . Then the solution to the RG flow equation (19) takes the simple linear form in  $x$ :

$$\frac{\Lambda}{\Lambda_c} = \frac{x_* - x}{x_* - x_0}, \quad (x_* = 8) \quad (21)$$

There are two cases to consider depending on whether the coupling is strong ( $x_0 < x_*$ ) or weak ( $x_0 > x_*$ ) at short distances. Based on the relation between  $x$  and hole doping described in section VI, we will refer to  $x_0 < x < x_*$  as the underdoped region and  $x_* < x < x_0$  as overdoped; in both cases  $\Lambda > 0$ . Furthermore, in order to clearly distinguish the two cases we will refer to  $x_0$  in the overdoped region as  $\tilde{x}_0$ . (What we refer to as the overdoped region is close but not identical to the usual terminology; the latter refers to the region beyond the maximum  $T_c$ .)

It is clear that our model is characterized by a single fundamental energy scale set by the cutoff  $\Lambda_c$ . Since  $\Lambda_c$  has units of a wave-vector  $\mathbf{k}$ , this energy scale is

$$E_0 = \hbar v_F \Lambda_c \equiv k_B T_0 \quad (22)$$

where  $\Lambda_c$  should be proportional to the inverse lattice spacing.

Before turning to mass renormalization, we now determine the 1-loop corrections to the anomalous dimension of the order parameters which are composite fields. Consider first the singlet operator  $\chi^- \chi^+$ . To first order in perturbation theory,

$$\langle \chi^- \chi^+(0) \dots \rangle = 8\pi^2 g \left[ \int \frac{d^3 \ell}{(2\pi)^3} \frac{1}{(\ell^2 + m^2)^2} \right] \langle \chi^- \chi^+(0) \dots \rangle \quad (23)$$

This contribution is cancelled by renormalizing the operator as follows:

$$\chi^- \chi^+ \rightarrow Z_{\chi^- \chi^+} \chi^- \chi^+ \quad (24)$$

where  $Z_{\chi^- \chi^+} = 1 + \delta Z_{\chi^- \chi^+}$  and

$$\delta Z_{\chi^- \chi^+} = -8\pi^2 g \int^\Lambda \frac{d^3 \ell}{(2\pi)^3} \frac{1}{(\ell^2 + m^2)^2} \quad (25)$$

The anomalous dimension  $\gamma_{\chi^- \chi^+}$  of  $\chi^- \chi^+$  is then

$$\gamma_{\chi^- \chi^+} = \Lambda \partial_\Lambda \log Z_{\chi^- \chi^+} = -4\hat{g} \quad (26)$$

where again we have assumed  $\Lambda \gg m$ . Repeating the above calculation for the  $SO(5)$  vector of order parameters one finds

$$\gamma_{\vec{\Phi}} = 4\hat{g} \quad (27)$$

Let  $[\mathcal{O}]$  denote the scaling dimension of  $\mathcal{O}$  at the fixed point, including the classical contribution of  $1/2$  for each  $\chi$  field. Using  $\hat{g}_* = 1/8$  at the fixed point, one obtains to 1-loop

$$[\chi^- \chi^+] \approx \frac{1}{2}, \quad [\vec{\Phi}] = [\chi^- \vec{\sigma} \chi^+] = [\chi_\uparrow^+ \chi_\downarrow^+] = [\chi_\downarrow^- \chi_\uparrow^-] \approx \frac{3}{2} \quad (28)$$

Thus one sees that the singlet is shifted down from the classical value, whereas the 5-vector of order parameters is shifted up. The above values agree exactly with the 1-loop approximation in the epsilon-expansion obtained in [3]. We point out that although the actual values of the fixed point value  $g_*$  and the functions  $\gamma(g)$  differ in the calculation performed here compared to the epsilon expansion, the results for the anomalous dimensions at the critical point agree to 1-loop. From the two-loop results obtained in [3], one sees that higher order corrections are reasonably small:  $[\chi^- \chi^+]$  changes to  $5/8$  and  $[\vec{\Phi}]$  actually remains at  $3/2$  at the next order.

Now we consider mass renormalization, which will be important in the sequel. The 1-loop correction to the self-energy shown in Figure 2 is a negative correction to  $m^2$ . This is cancelled by  $m^2 \rightarrow m^2(\Lambda) = m^2 + \delta m^2$  where

$$\delta m^2 = 8\pi^2 g \int^\Lambda \frac{d^3 \ell}{(2\pi)^3} \frac{1}{\ell^2 + m^2} \quad (29)$$

The  $m^2$  term on the RHS is extracted by taking a derivative with respect to  $m^2$  and then setting  $m^2 = 0$ :

$$\delta m^2 = 4gm^2/\Lambda \quad (30)$$

Defining

$$m = \Lambda \widehat{m} \quad (31)$$

one finds

$$\Lambda \partial_\Lambda \widehat{m}^2 = (-2 - 4\widehat{g}) \widehat{m}^2 \quad (32)$$

The  $-2\widehat{m}^2$  term simply corresponds to classical dimension 2 of  $m^2$  and  $4\widehat{g}$  the quantum correction. Since  $m^2$  is the coupling for  $\chi^- \chi^+$  this implies that the anomalous dimension of  $\chi^- \chi^+$  is  $-4\widehat{g}$ , in agreement with eq. (26).

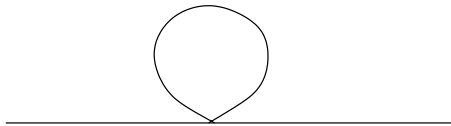


FIG. 2: One-loop correction to the self-energy.

## V. DYNAMICAL MASS GENERATION AND ITS IDENTIFICATION WITH THE PSEUDOGAP

Although the mass  $m$  is classically zero in the connection to the  $O(3)$  sigma model description of the Heisenberg AF described in section II, the operator  $\chi^- \chi^+$  is relevant and not forbidden by any symmetries so that in general it will be generated when one includes interactions. In this section we determine this dynamically generated mass to lowest order and propose that it be identified with the HTSC pseudogap.

If the original theory is massless, at 1-loop the correction to  $m^2$  coming from the diagram in Figure 2 is negative and equal to  $-8\pi^2 g \int \frac{d^3 \ell}{(2\pi)^2} \frac{1}{\ell^2}$ . Since the propagator  $1/\ell^2$  becomes  $1/(\ell^2 + m^2)$  when  $m \neq 0$ , a self-consistent equation for  $m$  is the following

$$m^2 = -8\pi^2 g \int \frac{d^3 \ell}{(2\pi)^3} \frac{1}{\ell^2 + m^2} \quad (33)$$

The one point function for the singlet is then

$$\langle \chi^- \chi^+ \rangle = -2 \int \frac{d^3 \ell}{(2\pi)^3} \frac{1}{\ell^2 + m^2} = \frac{m^2}{4\pi^2 g} \quad (34)$$

where we have used the equation (33). The two above equations can also be derived from a Hubbard-Stratanovich transformation based on the fact that the interaction is proportional to  $(\chi^- \chi^+)^2$ , as was done in [12].

In order to make sense of eq. (33) and obtain solutions, the mass renormalization discussed in section IV needs to be taken into account. Taking the limits of integration to be from zero to  $\Lambda$ , eq. (33) becomes

$$m^2 = -4g\Lambda + 4gm \tan^{-1} \Lambda/m \quad (35)$$

From eq. (29) with  $m = 0$  on the right hand side, one obtains  $\delta m^2 = 4g\Lambda$ , therefore the first term on the RHS above can be absorbed into  $m^2$ , and this is consistent with renormalization. The equation for  $m$  now becomes

$$\hat{m} = 4\hat{g} \tan^{-1} 1/\hat{m} \quad (36)$$

and has real solutions which are easily found numerically.

There are two useful analytic limits to the solution of eq. (36). When  $\hat{g}$  is large,  $\hat{m}$  is also large and the solution is approximately:

$$\hat{m} \approx 2\sqrt{\hat{g}}, \quad \langle \chi^- \chi^+ \rangle \approx \frac{\Lambda}{\pi^2} \quad (\hat{g} \text{ large}) \quad (37)$$

When  $\hat{g}$  is small,  $\hat{m}$  is also small and  $\tan^{-1} 1/\hat{m} \approx \pi/2$ . Thus in this limit one has

$$\hat{m} \approx 2\pi\hat{g}, \quad \langle \chi^- \chi^+ \rangle \approx g \quad (\hat{g} \text{ small}) \quad (38)$$

It is interesting to note that if one sends the cut-off to infinity in eq. (33) and performs the integral by analytic continuation in the spacetime dimension, then one obtains the solution (38). This means that the analog of dimensional regularization here overestimates  $\hat{m}$ , since by eq. (36),  $\hat{m} < 2\pi\hat{g}$ . In the underdoped region the approximation (37) is considerably better than (38) and we will use it in places below.

The mass  $m$  corresponds to an  $x$ -dependent energy scale

$$E_{pg}(x) = \hbar v_F m(x) \equiv k_B T^*(x) \quad (39)$$

where as before  $x = 1/\hat{g}$  and  $\hat{m}(x)$  is the solution to eq. (36). In units of the fundamental scale  $E_0$ :

$$\frac{E_{pg}}{E_0} = \frac{T^*}{T_0} = \hat{m}(x) \frac{\Lambda}{\Lambda_c} = \hat{m}(x) \frac{x_* - x}{x_* - x_0} \quad (40)$$

In the next section we will relate  $x$  to doping, thus the energy scale  $T^*$  is doping dependent. It should be emphasized that  $T^*$  simply corresponds to the temperature independent energy



scale  $E_{pg}$  and is thus not a real temperature; however as we will show in the sequel it can correspond to a cross-over scale in the real temperature.

A non-zero mass  $m$  clearly corresponds to a gap in the density of states since the 1-particle energies are  $E_{\mathbf{k}} = \sqrt{\mathbf{k}^2 + m^2}$ . We discuss this further at the end of this section. As a model of HTSC we thus identify the mass  $m$  with the pseudogap energy scale, i.e.  $m = E_{pg} = T^*$ . As we will show below, the thermodynamic properties of our model also support the identification of  $T^*$  with the HTSC pseudogap.

A plot of  $T^*$  verses  $x$  is shown in Figure 3. Note that  $T^*$  is close to linear near the critical point at  $x_* = 8$ . Furthermore, the pseudogap is smaller on the overdoped side. We point out that the re-appearance of the pseudogap on the overly doped side is contrary to what is normally observed.

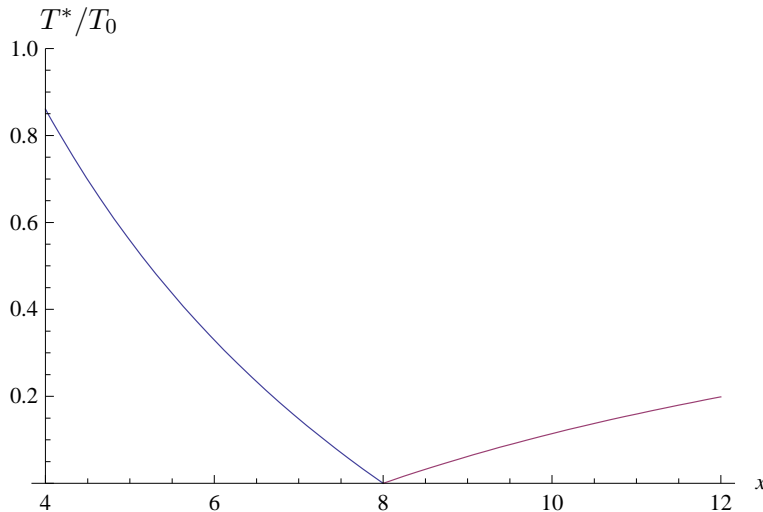


FIG. 3: The pseudogap  $T^*$  as a function of  $x$  for  $x_0 = 4$  and  $\tilde{x}_0 = 16$ .

Since the overall energy scale  $E_0$  depends both on  $v_F$  and  $\Lambda_c$ , in attempting to compare with the HTSC data it is more useful to fix  $E_0$  by using the pseudogap. It is known experimentally that at zero doping in the region of the AF phase  $E_{pg}$  is approximately the AF exchange energy  $J$ . Since zero doping occurs at  $x_0 = 0$  (see the next section), we can identify  $E_{pg}(x_0) = \hat{m}(x_0)E_0 \approx J$ . Since  $\hat{m}(x_0)$  is of order 1,  $E_0 \sim J$ . For the cuprates  $J/k_B \sim 1300 - 1400K$ .

An estimate of the density of states  $\rho(E)$  as a function of energy  $E$  can be obtained as follows. One has

$$\rho(k)dk = \frac{d^2\mathbf{k}}{(2\pi)^2} = \frac{kdk}{2\pi} = \rho(E)dE \quad (41)$$

If we approximate  $k$  in the above equation as the Fermi wave-vector  $k_F$ , then

$$\rho(E) \approx \frac{k_F}{2\pi} \left( \frac{dE}{dk} \right)^{-1} = \frac{k_F}{2\pi} \frac{1}{\sqrt{1 - m^2/E^2}} \quad (42)$$

This behavior is qualitatively shown in Figure 4.

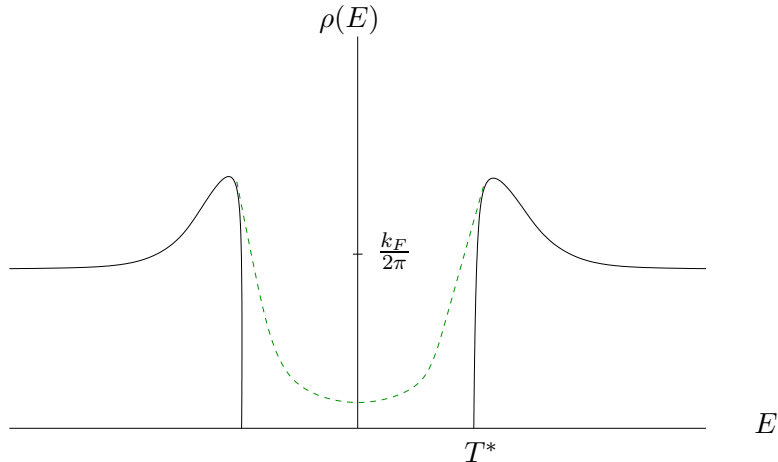


FIG. 4: Density of states as a function of energy  $E$ . The dotted line represents a sketch of what is measured using ARPES.

Angle-resolved photoemission (ARPES) measurements show a clear depression in the density of states and the leading edge of this depression is characterized by the pseudogap scale  $T^*$ . This behavior is shown schematically in Figure 4 as a dotted line. Thus one qualitative difference with what is observed is that the gap in our model is a clean one. Another difference is that due to the rotational invariance of our model, the pseudogap is isotropic, whereas the observed pseudogap shows lattice effects. It is anisotropic in the direction relative to the Fermi surface: the pseudogap is largest in the anti-nodal  $(0, \pi)$  direction and vanishes along “Fermi arcs” in the nodal  $(\pi, \pi)$  direction.

## VI. HOLE DOPING

Since renormalization removes degrees of freedom between  $\Lambda$  and  $\Lambda_c$ , this suggests that doping can be varied by varying the cutoff  $\Lambda$ . In [4] it was argued that a measure of hole doping can be defined based on the 1-point function  $\langle \chi^- \chi^+ \rangle$ . Since this one point function is proportional to  $\Lambda$  by dimensional analysis, we are led to identify doping  $p$  with

the dimensionless quantity

$$p = \frac{c}{\Lambda_c} (\langle \chi^- \chi^+ \rangle_{\Lambda_c} - \langle \chi^- \chi^+ \rangle_{\Lambda}) \quad (43)$$

for some constant  $c$ . In the underdoped regime, the 1-point function is approximately given by eq. (37):

$$p(x) \approx \frac{c}{\pi^2} \left( 1 - \frac{\Lambda}{\Lambda_c} \right) = \frac{c}{\pi^2} \left( \frac{x - x_0}{x_* - x_0} \right) \quad (44)$$

where we have used eq. (21). Half-filling then corresponds to  $\Lambda = \Lambda_c$ , i.e.  $x = x_0$ . Thus, in the approximation we have made, plots of various physical properties as a function of doping  $p$  is simply related to plots as a function of the inverse coupling  $x$  by rescaling and shift of the  $x$ -axis. We choose to plot against  $x$  since this more clearly reveals the RG properties.

We can give a rough estimate of the constant  $c$  following an argument made in [4]. Consider a lattice fermion model where  $\vec{S}_{\mathbf{x}}$  is the local spin variable at lattice site  $\mathbf{x}$ , which is bilinear in the fermion operators. One has

$$\vec{S} \cdot \vec{S} = -\frac{3}{2} n_{\uparrow} n_{\downarrow} + \frac{3}{4} (n_{\uparrow} + n_{\downarrow}) \quad (45)$$

where  $n_{\uparrow, \downarrow}$  is the number of fermions of spin up or down at each site. From this relation one sees that at half-filling  $n_{\uparrow} n_{\downarrow} = 0$ ,  $n_{\uparrow} + n_{\downarrow} = 1$  and  $\vec{S}^2 = 3/4$ , i.e.  $\vec{S}$  is constrained to be a spin  $\frac{1}{2}$  vector and the model can be mapped onto the Heisenberg model. Dividing the above equation by the volume squared and taking the infinite volume limit, one finds that the right hand side is  $-\frac{3}{2} \rho_{\uparrow} \rho_{\downarrow}$  where  $\rho_{\uparrow, \downarrow}$  are number densities.

In our continuum model,  $\vec{S}$  is represented by the bilinear  $\vec{\phi}$  and one has the identity:

$$\vec{\phi} \cdot \vec{\phi} = -\frac{3}{2} (\chi^- \chi^+)^2 \quad (46)$$

Comparing with the continuum limit of eq. (45), one identifies  $\chi^- \chi^+ = (\rho_{\uparrow} + \rho_{\downarrow})/\sqrt{2}$ , which corresponds to  $c = \sqrt{2}$ . At the critical point this gives  $p_{\text{crit}} \approx .14$ . Since this is only a rough estimate, one can alternatively fix  $c$  in principle by fitting to experimental data.

## VII. SPECIFIC HEAT

An approximation to the specific heat can be made based on including just the effects of the dynamically generated mass. A gas of 4 types of fermionic particles with single particle

energies  $\omega_{\mathbf{k}} = \sqrt{\mathbf{k}^2 + m^2}$  has the free energy per volume at temperature  $T$ :

$$\mathcal{F} = -4T \int_0^{\Lambda_c} \frac{d^2\mathbf{k}}{(2\pi)^2} \log(1 + e^{-\omega_{\mathbf{k}}/T}) \quad (47)$$

One easily sees that  $\mathcal{F}/\Lambda_c^3$  is a function of the two dimensionless variables  $T/T_0$  and  $T/T^*$  where as in section V we have identified  $T^* = m$ .

At very low temperatures  $T \ll T_0$  we can approximate the log as  $e^{-\omega_{\mathbf{k}}/T}$  and effectively send the cut-off  $\Lambda_c$  to infinity, and  $\mathcal{F}/T^3$  becomes a scaling function of  $T^*/T$ . The result is

$$\mathcal{F} \approx -\frac{2T^3}{\pi} e^{-T^*/T} \left(1 + \frac{T^*}{T}\right) \quad (48)$$

The entropy density is then:

$$S = -\frac{\partial \mathcal{F}}{\partial T} \approx \frac{3T^2}{\pi} e^{-T^*/T} \left(1 + \frac{T^*}{T} + \frac{1}{3} \left(\frac{T^*}{T}\right)^3\right) \quad (49)$$

and the specific heat:

$$C = -T \frac{\partial^2 \mathcal{F}}{\partial T^2} \approx \frac{12T^2}{\pi} e^{-T^*/T} \left(1 + \frac{T^*}{T} + \frac{1}{2} \left(\frac{T^*}{T}\right)^2 + \frac{1}{2} \left(\frac{T^*}{T}\right)^3\right) \quad (50)$$

It is convenient to define the quantity  $\gamma = C/T$  since for a Fermi liquid  $\gamma$  is a constant. The primary feature of our model is that  $\gamma \propto T$  at very low temperatures compared to  $T^*$  and  $T_0$ , which is ultimately attributed to the relativistic nature of the model.

At higher temperatures there is a crossover to a different behavior. Since  $\Lambda_c$  can be scaled out of the eq. (47), the cross-over temperature is the pseudogap temperature  $T^*$ . Below we plot the entropy and  $\gamma$  as a function  $T$  for various ‘‘doping’’  $x$ . The plots are in terms of the dimensionless quantities  $T/T_0$ ,  $S/\Lambda_c^2$  and  $\gamma/\Lambda_c$ . One clearly sees the crossover at  $T = T^*$ .

Experimental data for  $\gamma$  is shown in Figure 7. In comparing with our results, it is important to bear in mind that the data contains contributions from the quasi-particle excitations in the SC phase, which explains the peaks to the left, and such effects are not included in our calculation. Thus, our curves should be compared with the data to the right of the SC peaks. At temperatures below  $T_0$  one sees a reasonably good qualitative agreement with the behavior computed above: for  $T \ll T^*$ ,  $\gamma \propto T$ , with a crossover to a different behavior at  $T^*$ . The dependence on doping is also qualitatively correct, i.e. the peaks of the curves move toward the left with increased doping. One difference is that whereas our computed  $\gamma$  goes to zero at high temperature, the experiments indicate that

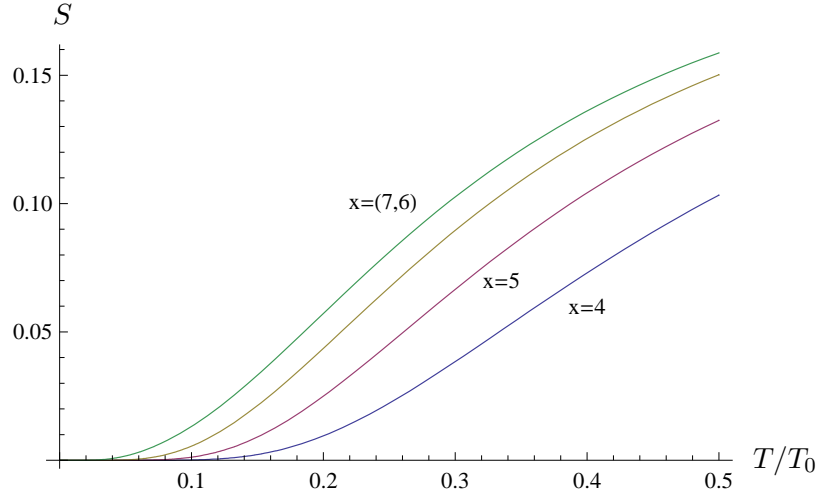


FIG. 5: Entropy as a function of temperature for  $x_0 = 4$ . The vertical axis is the dimensionless quantity  $S/E_0^2$ .

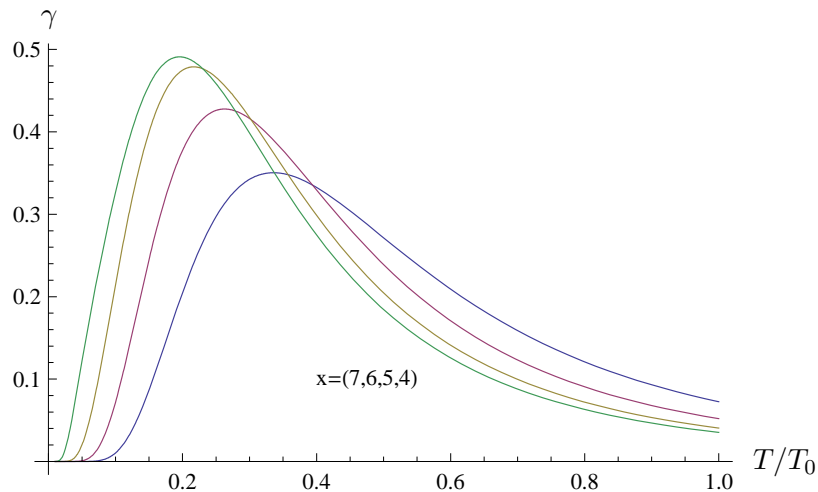


FIG. 6:  $\gamma = C/T$  as a function of temperature at various “doping”  $x$  for  $x_0 = 4$ . The larger amplitude curves correspond to larger doping. The vertical axis is the dimensionless quantity  $\gamma/E_0$ .

at high temperatures  $\gamma$  approaches the Fermi-liquid result, i.e.  $\gamma$  approaches a constant. Our model of course does not crossover to a Fermi liquid at high temperatures, because as explained in section III it is expected to break down at high enough temperatures, so at best it may describe temperatures up to and above  $T^*$ .

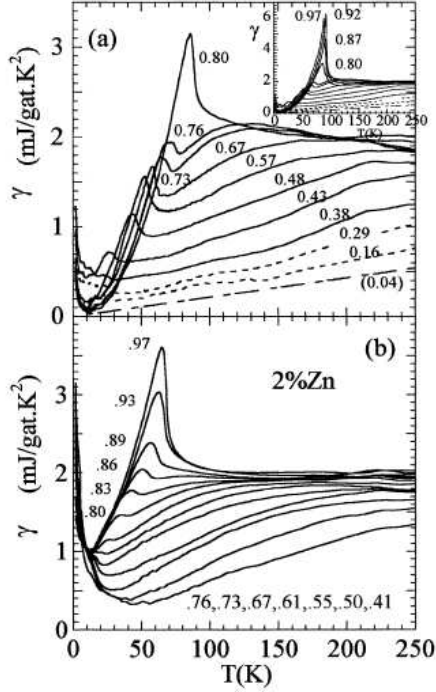


FIG. 7: Experimental data for  $\gamma(T)$  for  $Y_{0.8}Ca_{0.2}Ba_2Cu_3O_{6+x}$  (from [9]).

### VIII. NON-ZERO MAGNETIC FIELD

In this section we compute the spin response to a magnetic field and also the magnetic field dependence of the specific heat in the same approximation we made in the last section, i.e. we only consider the effects of the dynamically generated mass. Both these quantities can be studied by adding a term to the action  $\int d^2\mathbf{x}dt \sqrt{2}\vec{h} \cdot \vec{\phi}$ . Comparing with the calculation of the effective potential  $V_{\text{eff}} = \mathcal{F}$  in [4], one sees that the free energy at zero temperature is

$$\mathcal{F} = - \int \frac{d\omega d^2\mathbf{k}}{(2\pi)^3} \log((\omega^2 + \omega_{\mathbf{k}}^2)^2 - h^2) \quad (51)$$

where as before,  $\omega_{\mathbf{k}}^2 = \mathbf{k}^2 + m^2$ .

## A. Spin response

The one point function  $\langle \vec{\phi} \rangle$  in the presence of  $\vec{h}$  can be obtained from the first derivative of the logarithm of the partition function  $Z = \exp(-\mathcal{F}V/T)$  where  $V$  is the volume. For a single component of  $\vec{\phi}$ , one obtains

$$\langle \phi \rangle = \frac{1}{\sqrt{2}} \frac{\partial \mathcal{F}}{\partial h} = \frac{1}{\sqrt{2}} \int \frac{d\omega d^2\mathbf{k}}{(2\pi)^3} \left( \frac{1}{\omega^2 + \omega_{\mathbf{k}}^2 - h} - \frac{1}{\omega^2 + \omega_{\mathbf{k}}^2 + h} \right) \quad (52)$$

At finite temperature  $T$ ,  $\omega$  becomes a quantized Matsubara frequency  $\omega = 2\pi\nu T$  where  $\nu \in Z + 1/2$  and one makes the replacement:

$$\int \frac{d\omega}{2\pi} \rightarrow T \sum_{\nu \in Z+1/2} \quad (53)$$

We need the identity

$$T \sum_{\nu \in Z+1/2} \frac{1}{a^2 + (2\pi\nu T)^2} = \frac{1}{2a} \tanh\left(\frac{a}{2T}\right) \quad (54)$$

This gives

$$\langle \phi \rangle = \frac{1}{2\sqrt{2}} \int \frac{d^2\mathbf{k}}{(2\pi)^2} \left( \frac{1}{\sqrt{\omega_{\mathbf{k}}^2 - h}} \tanh \frac{\sqrt{\omega_{\mathbf{k}}^2 - h}}{2T} - (h \rightarrow -h) \right) \quad (55)$$

The linear response for small  $h$  follows from Taylor expanding the integrand:

$$\langle \vec{\phi} \rangle = \chi_s(m, T) \vec{h} \quad (56)$$

where

$$\chi_s(m, T) = \frac{1}{4\sqrt{2}T} \int \frac{d^2\mathbf{k}}{(2\pi)^2} \frac{1}{\omega_{\mathbf{k}}^2} \left( \tanh^2 \frac{\omega_{\mathbf{k}}}{2T} + \frac{2T}{\omega_{\mathbf{k}}} \tanh \frac{\omega_{\mathbf{k}}}{2T} - 1 \right) \quad (57)$$

Plots of  $\chi_s$  as a function of temperature are shown in Figure 8. One sees that the spin response is quenched when  $T < T^*$ , consistent with experiments.

## B. Specific heat

Define

$$\Delta \mathcal{F} = \mathcal{F}(h) - \mathcal{F}(0) \quad (58)$$

Integrating the identity eq. (54) one can show

$$T \sum_{\nu \in Z+1/2} (\log(\omega_{\nu}^2 + \omega_{\mathbf{k}}^2 - h) - \log(\omega_{\nu}^2 + \omega_{\mathbf{k}}^2)) = 2T \log \left( \frac{1 + e^{-\sqrt{\omega_{\mathbf{k}}^2 - h}/T}}{1 + e^{-\omega_{\mathbf{k}}/T}} \right) + \sqrt{\omega_{\mathbf{k}}^2 - h} - \omega_{\mathbf{k}} \quad (59)$$

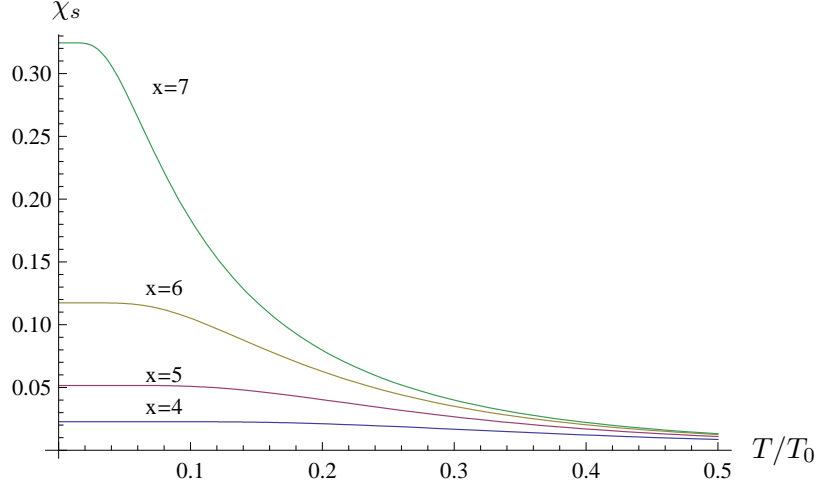


FIG. 8: The spin response as a function of temperature at various doping variable  $x$  for  $x_0 = 4$ . The vertical axis corresponds to the dimensionless quantity  $\chi_s \cdot E_0$ .

Therefore up to a constant that is independent of  $T$  and does not affect the specific heat:

$$\Delta\mathcal{F} = -2T \int \frac{d^2\mathbf{k}}{(2\pi)^2} \log \left( \frac{(1 + e^{-\sqrt{\omega_{\mathbf{k}}^2 - h/T})(1 + e^{-\sqrt{\omega_{\mathbf{k}}^2 + h/T})}}{(1 + e^{-\omega_{\mathbf{k}}/T})^2} \right) \quad (60)$$

One can then define

$$\Delta\gamma = -\frac{\partial^2 \Delta\mathcal{F}}{\partial T^2} \quad (61)$$

Plots of  $\Delta\gamma$  as a function of  $T$  for different  $x, h$  are shown in Figures 9, 10. (These plots are in arbitrary units since we have not specified the strength of the magnetic field.) At very small  $h$ ,  $\Delta\gamma \propto h^2$ .

## IX. FINITE TEMPERATURE D-WAVE GAP EQUATION AND THE EFFECT OF THE PSEUDOGAP.

### A. Zero temperature

It was shown in [4] that the 1-loop corrections to scattering of Cooper pairs leads to a d-wave superconducting gap of the form

$$q(\mathbf{k}) = \delta^2(k_x^2 - k_y^2) = \delta^2 k^2 \cos(2\theta) \quad (62)$$

where  $q(\mathbf{k})$  is a Fourier transform of Cooper pairing order parameters  $\langle \chi_{\uparrow}^{\pm}(\mathbf{x}_1) \chi_{\downarrow}^{\pm}(\mathbf{x}_2) \rangle$ . Before turning to the main topic, some remarks on the d-wave property of the gap are called



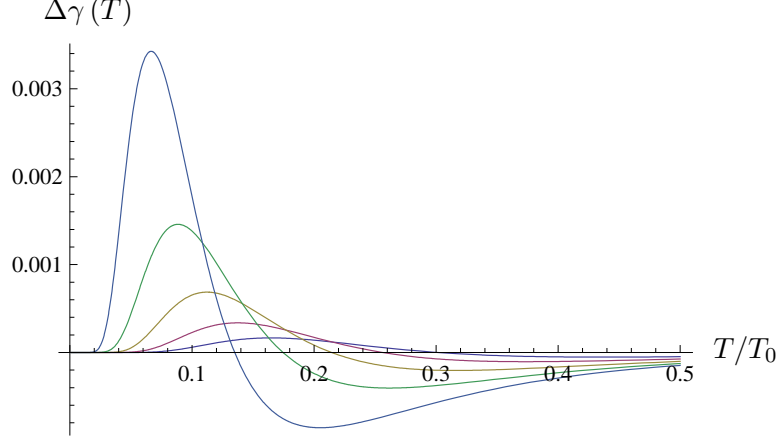


FIG. 9:  $\Delta\gamma(h, T)$  evaluated at  $x = 4, 4.5, 5, 5.5, 6$  for  $x_0 = 4$  as a function of temperature for fixed  $h = 0.025$ . The larger amplitude curves correspond to larger  $x$ , i.e. larger doping.

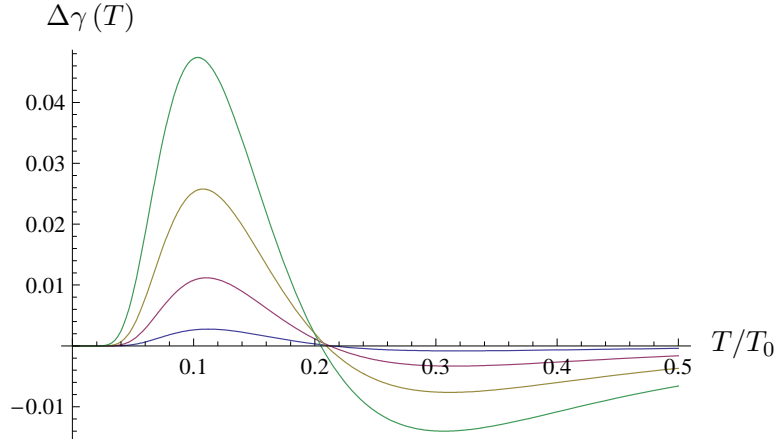


FIG. 10:  $\Delta\gamma(h, T)$  as a function of temperature for various  $h = 0.05, 0.1, 0.15, 0.2$  (increasing  $h$  corresponds to increasing amplitudes on the plot) at fixed  $(x, x_0) = (5, 4)$ .

for. Since the d-wave gap equation derived in [4] was based on a rotationally invariant hamiltonian, the most general solution involves a rotation by an arbitrary angle  $\theta_0$ , i.e.  $\cos 2\theta \rightarrow \cos 2(\theta - \theta_0)$  in the above equation. On the other hand in HTSC the lattice breaks the rotational symmetry and the d-wave gap is oriented with respect to the Fermi surface in a specific way, namely the gap vanishes in the nodal direction  $(k_x, k_y) = (\pi, \pi)$ , which corresponds to  $\theta_0 = 0$ . This can be reconciled as follows. Free particles on the lattice have dispersion relation  $\varepsilon_{\mathbf{k}} = -2(\cos k_x + \cos k_y)$ . Thus the Fermi surface has the symmetry  $k_x \rightarrow -k_x$ . Requiring this symmetry fixes  $\theta_0 = 0$ .

In this sub-section we study the effect of the non-zero mass  $m$  on the zero temperature d-wave superconducting gap equation. The effect of the mass term is simply the shift  $\omega^2 \rightarrow \omega^2 + m^2$  and the d-wave gap equation derived in [4] becomes:

$$\delta^4 = 2g_2 \int d\omega dk^2 \left( 1 - \frac{\omega^2 + k^2 + m^2}{\sqrt{(\omega^2 + k^2 + m^2)^2 + \delta^4 k^4}} \right) \quad (63)$$

where  $k^2 = \mathbf{k}^2$ . The coupling  $g_2$  comes from the 1-loop scattering of Cooper pairs and is given by

$$g_2 = \frac{8\pi^2 g^2}{5} \int \frac{d^3 \ell}{(2\pi)^3} \frac{1}{(\ell^2 + m^2)^4} \quad (64)$$

For simplicity we incorporate the cut-off as follows:  $|\omega| < \infty$  and  $k^2 < \Lambda_c^2$  which is more appropriate for comparison with the finite temperature version we consider below.

Re-expressing the gap equation in terms of dimensionless quantities by rescaling  $k \rightarrow \Lambda_c k$  and  $\omega \rightarrow \Lambda_c \omega$ , one obtains

$$\delta^4 = 2\hat{g}_2 \int_0^\infty d\omega \int_0^1 dk^2 \left( 1 - \frac{\omega^2 + k^2 + m'^2}{\sqrt{(\omega^2 + k^2 + m'^2)^2 + \delta^4 k^4}} \right) \quad (65)$$

where  $m' = m/\Lambda_c$  and  $\hat{g}_2 = g_2 \Lambda_c^3$ .

Since eq. (64) is ultra-violet convergent, it can be approximated by letting the upper cut-off go to infinity, giving  $g_2 = \pi g^2/40m^5$ . Incorporating the RG prescriptions of section IV,  $g = \Lambda \hat{g}$  and  $m = \Lambda \hat{m}$ , one finds that the parameters in the gap equation (65) are the following:

$$\hat{g}_2 = \frac{\pi}{40} \frac{\hat{g}^2}{\hat{m}^5} \left( \frac{\Lambda_c}{\Lambda} \right)^3, \quad m' = \frac{\Lambda}{\Lambda_c} \hat{m} \quad (66)$$

where the ratio  $\Lambda/\Lambda_c$  is given in eq. (21). Finally, since under a RG transformation  $\delta k \rightarrow \delta \Lambda k/\Lambda_c \equiv \delta' k$ , the physical gap in the theory at RG scale  $\Lambda$  is  $\delta' = \Lambda \delta/\Lambda_c$ . The  $x$ -dependence of the solutions  $\delta$  arises from the  $x$ -dependence of  $\hat{g}_2$  and  $m'$ . A plot of  $\delta'$  as a function of  $x$  is shown in Figure 11. It is important to point out that the interpretation of the critical point at  $x_*$  presented here differs from the original proposal in [4], in that in the present work we extend  $x$  beyond  $x_*$  by introducing  $\tilde{x}_0$ , and this places the maximum value of the gap near the critical point  $x_* = 8$ . (We have effectively patched together what was referred to as Type A and B in [4].) Further justification for this location of the critical point is based on the calculation of  $T_c$ , which reaches a maximum value near the critical point, as explained below.

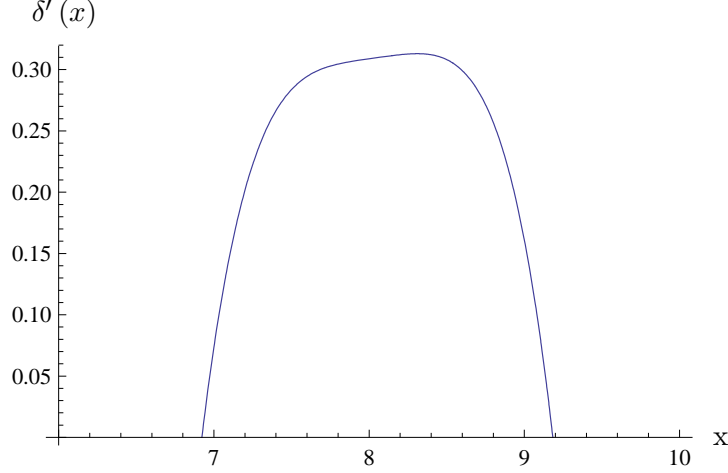


FIG. 11: Plot of  $\delta'_q(x)$  vs  $x$  for  $x_0 = 4$  and  $\tilde{x}_0 = 12$ .

One can easily verify numerically that the pseudogap competes with SC in the following sense: if one artificially increases the mass  $m$ , then the value of the gap  $\delta$  decreases, and eventually vanishes for  $m$  too large. (This was shown already in [4].)

## B. Finite temperature

In order to derive the finite temperature version of the above d-wave gap equation, we start with the un-integrated form derived in [4]:

$$q(\mathbf{k}) = - \int \frac{d\omega d^2\mathbf{k}'}{(2\pi^3)} G(\mathbf{k}, \mathbf{k}') \frac{q(\mathbf{k}')}{(\omega^2 + \omega_{\mathbf{k}'}^2)^2 + q(\mathbf{k}')^2} \quad (67)$$

where the kernel is

$$G(\mathbf{k}, \mathbf{k}') = -8\pi^2 g_2 k^2 k'^2 \cos 2(\theta - \theta') \quad (68)$$

The equation (63) is obtained upon performing the angular integral.

At finite temperature,  $\omega$  becomes a quantized Matsubara frequency  $\omega_\nu = 2\pi T\nu$ , where  $T$  is the temperature and  $\nu$  is a half-integer, i.e.  $\nu \in Z + 1/2$ . As before, the integral  $\int d\omega/2\pi$  is replaced with  $T \sum_\nu$ . One needs the identity:

$$T \sum_\nu \frac{1}{(\omega_\nu^2 + \omega_{\mathbf{k}}^2)^2 + q^2} = \frac{T}{q} \text{Im} \sum_\nu \frac{1}{\omega_\nu^2 + \omega_{\mathbf{k}}^2 - iq} = \frac{1}{q} \text{Im} \left( \frac{1}{2\omega_{\mathbf{k},q}} \tanh \left( \frac{\omega_{\mathbf{k},q}}{2T} \right) \right) \quad (69)$$

where  $\omega_{\mathbf{k},q} = \sqrt{\omega_{\mathbf{k}}^2 - iq}$ .

Due to the specific form of the kernel  $G$ , the solution to the equation (67) is of the d-wave form (62) (up to an arbitrary rotation) where  $\delta$  satisfies the integral equation

$$\delta^2 = g_2 \int dk d\theta k^3 \cos(2\theta) \text{Im} \left( \frac{1}{\omega_{\mathbf{k},\delta}} \tanh \left( \frac{\omega_{\mathbf{k},\delta}}{2T} \right) \right) \quad (70)$$

where

$$\omega_{\mathbf{k},\delta} = \sqrt{\omega_{\mathbf{k}}^2 - i\delta^2 k^2 \cos 2\theta} \quad (71)$$

Finally, the physical temperature at the scale  $\Lambda$  follows from the RG transformation  $T \rightarrow T\Lambda/\Lambda_c$ .

Solutions of the above equation are  $\delta(x, T)$ . One can easily verify numerically that as the temperature goes to zero, one recovers the solution  $\delta(x)$  to the zero temperature gap equation (65). One also finds that as the temperature is raised there are no solutions to the above equation for  $T > T_c$  and this defines the  $x$ -dependent critical temperature  $T_c$ . This is shown in Figure 12.

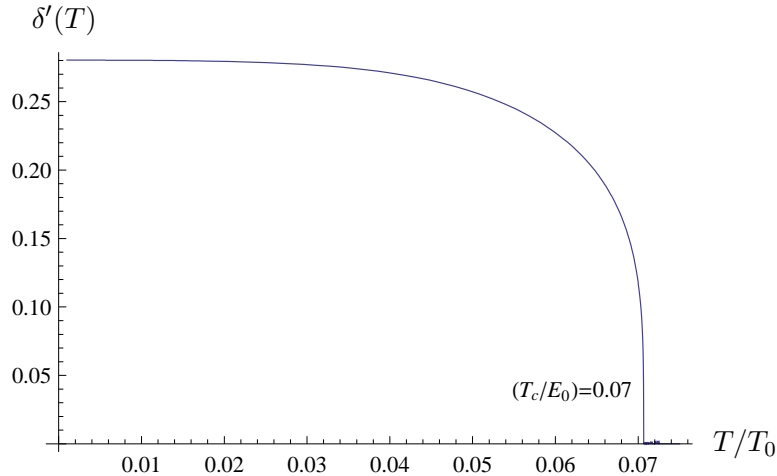


FIG. 12: The d-wave gap  $\delta'(T)$  as a function of  $T$  for  $x = 7.5, x_0 = 4$ .

The critical temperature  $T_c$  as a function of  $x$  on both sides of  $x_*$  are shown in Figure 13. It turns out that  $T_c$  at the critical value  $x = x_*$ , i.e.  $T_c^* = T_c(x_*)$ , is universal in that it only depends on the overall scale  $T_0$  and not on  $x_0, \tilde{x}_0$  since the scale factor  $\Lambda/\Lambda_c$  vanishes at this point. Using the estimated relation between  $x$  and doping in section VI, the critical point occurs at doping  $p_{\text{crit}} \approx .14$ . The dome shape of  $T_c$  is a property of the mathematical structure of the gap equation and nothing universal is happening at the termination points

of SC on either side of the critical point. Numerically we find that at the critical point

$$\frac{T_c^*}{T_0} \approx .084, \quad \frac{T_c^*}{T_0 \delta'(x_*)} \approx .268 \quad (72)$$

We also find numerically that the maximum value of  $T_c$  occurs close to the critical point so that  $T_c^{\max} \approx .084T_0$ , i.e.  $T_c^{\max}$  is simply proportional to fundamental energy scale  $E_0$ .

As argued in section V,  $T_0$  should be identified with the anti-ferromagnetic exchange energy  $J$  at half-filling. For  $T_0 = 1350K$ , this gives  $T_c^{\max} \approx 113K$ , which is quite reasonable for HTSC. It should be emphasized that the above  $T_c$  is intrinsic to the two spatial dimensions, i.e. does not involve any kind of inter-planar energy scales.

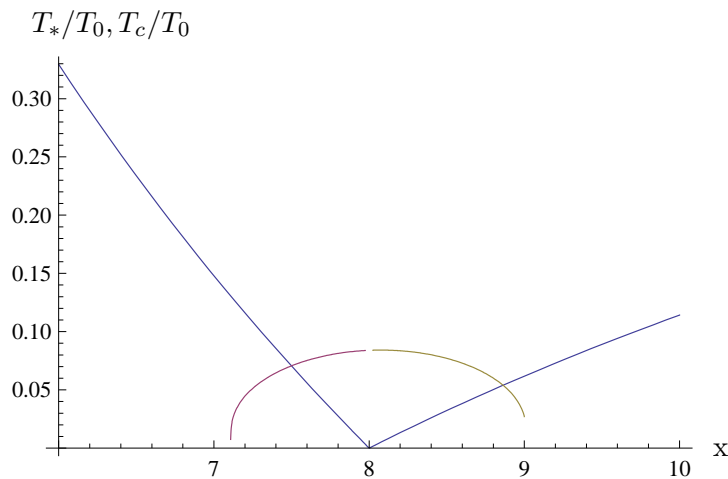


FIG. 13: Plot of  $T_c$  and  $T_*$  vs  $x$  for  $x_0 = 4$  and  $\tilde{x}_0 = 12$ .

## X. CONCLUDING REMARKS

In summary, we have further developed the interacting symplectic fermion model in two spatial dimensions by studying a dynamically generated relativistic mass and by including a finite temperature. This allowed us to study some fundamental properties of the model, such as the specific heat and spin response, which clearly show non-Fermi liquid properties. As a simplified model of HTSC, we identified the pseudogap energy scale with the zero temperature relativistic mass  $m$ , and pointed out some close parallels with the observed phenomenology of the pseudogap.

We studied the effects of the pseudogap and finite temperature on the d-wave gap equation. In this model, the pseudogap clearly competes with superconductivity as a distinct

phenomenon. Our analysis of  $T_c$  suggests that the quantum critical point of our model, where the pseudogap vanishes, occurs inside the superconducting dome near optimal doping. For an antiferromagnetic exchange energy of  $J \sim 1350K$ , solutions of the d-wave gap equation give a maximum  $T_c$  of about  $110K$ .

## XI. ACKNOWLEDGMENTS

We would like to thank Ian Affleck, Denis Bernard, Dean Robinson, Henry Tye, and Jan Zaanen for discussions. This work is supported by the National Science Foundation under grant number NSF-PHY-0757868. EK would also like to acknowledge the support of the National Defense Science and Engineering Graduate Fellowship of the American Society for Engineering Education.

- 
- [1] R. Shankar, Rev. Mod. Phys. **66** (1994) 129;
  - [2] A. LeClair, arXiv:cond-mat/0610639,0610816.
  - [3] A. LeClair and M. Neubert, JHEP **10** (2007) 027.
  - [4] E. Kapit and A. LeClair, J. Phys. A. **42**, 025402 (2009) [arXiv:0805.4182]; arXiv:0805.2951.
  - [5] S. C. Zhang, Science **275** (1997) 1089.
  - [6] P. A. Lee, N. Nagosa, and X.-G. Wen, Rev. Mod. Phys. **78**, 17 (2006).
  - [7] M.R. Norman and C. Pepin, arxiv:cond-mat/0302347.
  - [8] M. R. Norman, D. Pines, and C. Kallin, Adv. Phys. **54**, 715 (2005)
  - [9] J. W. Loram, K. A. Mirza, J. R. Cooper and J. L. Tallon, J. Phys. Chem. Solids Vol **59** (1998) 2091; J. W. Loram, J. Luo, J. R. Cooper, W. Y. Liang and J. L. Tallon, J. Phys. Chem. Solids Vol **62** (2001) 59; J. L. Luo, J. W. Loram, T. Xiang, J. R. Cooper and J. L. Tallon, arXiv:cond-mat/0112065.
  - [10] J. L. Tallon and J. W. Loram, arXiv:cond-mat/0005063.
  - [11] S. Hufner, M.A. Hossain, A. Damascelli and G. A. Sawatzky, Rep. Prog. Phys. **71** (2008) 062501.
  - [12] H. Tye, arXiv:0804.4200.
  - [13] X. J. Zhou et. al. Nature **423** (2003) 398.

- [14] D. Robinson, E. Kapit and A. LeClair, to appear.
- [15] C. M. Bender, Rev. Mod. Phys. **70** (2007) 947 [hep-th/0703096].
- [16] A. Mostafazadeh, J. Math. Phys. **43** (2002) 205.
- [17] S. Guruswamy and A. W. W. Ludwig, Nucl. Phys. **B519** (1998) 661 [arXiv:hep-th/9612172].
- [18] F. D. M. Haldane, Phys. Lett. **93A** (1983) 464; Phys. Rev. Lett. **50** (1983) 1153.
- [19] I. Affleck, Les Houches lectures 1988, North-Holland.